

Dielectric-loaded surface plasmon-polariton waveguides at telecommunication wavelengths: Excitation and characterization

Tobias Holmgaard^{a)} and Sergey I. Bozhevolnyi

Department of Physics and Nanotechnology, Aalborg University, Skjernvej 4A, DK-9220 Aalborg Øst, Denmark

Laurent Markey and Alain Dereux

Institut Carnot de Bourgogne, UMR 5209 CNRS-Université de Bourgogne, 9 Av. A. Savary, BP 47 870, F-21078 Dijon Cedex, France

(Received 17 October 2007; accepted 28 November 2007; published online 9 January 2008)

The excitation and propagation of strongly confined surface plasmon-polariton (SPP) waveguide modes, supported by 500-nm-wide and 550-nm-high dielectric ridges fabricated on smooth gold films, are investigated at telecommunication wavelengths using a scanning near-field optical microscope. Different tapering structures for coupling of SPPs, excited at bare gold surfaces, into dielectric-loaded SPP waveguide (DLSPW) modes are considered. The DLSPW mode confinement and propagation loss are characterized. The DLSPW mode propagation along an S bend having the smallest curvature radius of 2.48 μm is shown, demonstrating the potential of DLSPW technology for the realization of high-density photonic integrated circuits. © 2008 American Institute of Physics. [DOI: 10.1063/1.2825588]

Ever increasing demands for high-density photonic integrated circuits impel the search for waveguide configurations ensuring strong (lateral) mode field confinement, which is a prerequisite for realizing efficient and compact bends, splitters, and other waveguide components. For this reason, surface plasmon polaritons (SPPs) have attracted great interest in recent years.¹ SPPs are surface electromagnetic modes propagating along a metal-dielectric interface. They feature a maximum of the electric field at the interface and decay exponentially away from it.² A variety of SPP waveguide structures such as two dimensional SPP band gaps,³ metal stripes,⁴⁻⁶ and V grooves in a metal surface⁷⁻⁹ have been proposed and investigated. An alternative and technologically simple strategy for achieving tight SPP mode confinement exploits the dependence of the SPP propagation constant on the refractive index of the dielectric at the metal-dielectric interface by depositing dielectric ridges on the metal surface. The resulting configuration, known as dielectric-loaded SPP waveguides (DLSPWs), has been demonstrated experimentally at the free space wavelengths $\lambda=800$ nm (Refs. 10 and 11) and $\lambda=1520$ nm.¹² Numerical analysis of DLSPWs at telecommunication wavelengths^{13,14} showed prospects for obtaining very low radiation losses at compact bends and splitters provided that the ridges used are sufficiently high and narrow to ensure both large index contrast and strong field confinement in the single-mode propagation. In the present work, highly confined DLSPW modes are demonstrated experimentally by near-field optical characterization of straight DLSPW ridges and S bends at telecommunication wavelengths.

The waveguide dimensions, i.e., ridge height and width, are deduced by simultaneously considering mode confinement and propagation loss, while retaining the demand of single mode DLSPWs. It is advantageous to choose a ridge as high as allowed by the single mode condition, as both lateral confinement and propagation length increases with

ridge height (true only for ridges higher than ~ 300 nm).¹³ Decreasing the ridge width initially has the effect of squeezing the field laterally, thereby achieving better mode confinement. However, at a certain width the field can no longer be confined to the ridge and spreads out into the surrounding air. At telecommunication wavelengths, these considerations led to the determined optimum ridge height $h=600$ nm and width $w=500$ nm.¹³

The investigated sample consists of poly-methylmethacrylate (PMMA) ridges ($n_r=1.493$) deposited on a 50-nm-thick gold film by utilizing deep ultraviolet lithography. A thin glass substrate supports the metal film and the dielectric waveguides.

A funnel structure has been designed and realized in order to efficiently couple the SPPs excited at the gold-air interface by total internal reflection into bound DLSPW modes. Moreover, close to the waveguide, this tapering structure may screen the propagation of the incident gold-air interface SPPs. Four tapering dimensions have been realized in order to determine the optimum structure for coupling SPPs into DLSPW modes [Fig. 1(a)]. In the four designs, the initial funnel width is kept constant (10 μm) and the length is varied from 10 to 25 μm by steps of 5 μm , thereby varying funnel angles. The width of the fabricated waveguides has been investigated by scanning electron microscopy (SEM) and found to be $w\sim 500$ nm [Fig. 1(b)]. An atomic force microscope (AFM) has determined the height of the ridges to be $h\sim 550$ nm [Figs. 1(c) and 1(d)]. The measured waveguide characteristics are in good agreement with the targeted optimum values. Furthermore, the dielectric waveguides are generally found to be of high quality with only very small variations in width and height.

To characterize DLSPW components at telecommunication wavelengths, the experimental setup consists of a scanning near-field optical microscope (SNOM) where SPPs are excited at the gold-air interface in the Kretschmann-Raether configuration.² Once the sample is placed in the SNOM setup, an immersion oil matches the index between

^{a)}Electronic mail: holmgaard@nano.aau.dk.

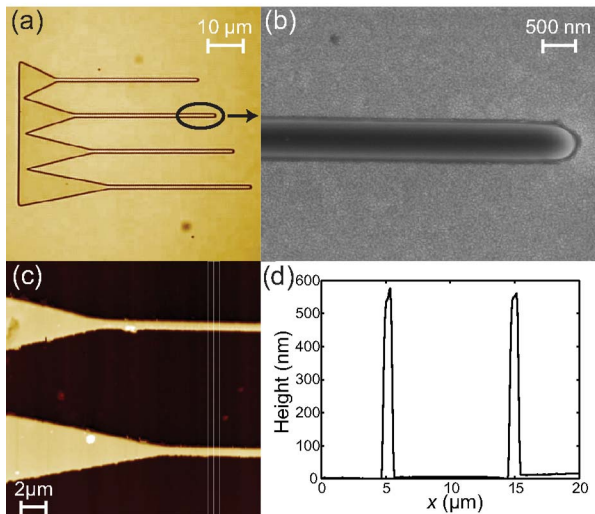


FIG. 1. (Color online) (a) Microscope image of a block with four waveguides with in coupling funnel of different dimensions. (b) SEM image of the termination region of a straight waveguide, revealing a waveguide width of ~ 500 nm. (c) AFM image of the tapering region and (d) cross section of the AFM image revealing a waveguide height of ~ 550 nm.

the prism and the sample substrate. Using a lensed fiber, an incident Gaussian beam is focused on the gold film to a spot size of $\sim 15 \mu\text{m}$. The adjustment of the incident angle is performed by minimizing the reflected signal recorded with a charge-coupled device camera. An uncoated etched fiber tip is scanned over the sample by means of a feedback loop, yielding both topographic and near-field optical images of the investigated area. SPPs are excited outside the funnel at the gold-air interface and propagate from top to bottom in the reported near-field images.

The DLSPW block with four tapering designs [Fig. 1(a)] has been investigated in order to determine the in-coupling efficiency of the different funnel dimensions [Fig. 2]. The funnels show increasing in-coupling efficiency with decreasing funnel angle, and the scattering of SPPs at the tapering-waveguide transition is clearly weaker in the $10 \times 25 \mu\text{m}$ funnel [Fig. 2(a)] as compared to the $10 \times 10 \mu\text{m}$ funnel [Fig. 2(d)]. Thus, the longest and smoothest transition

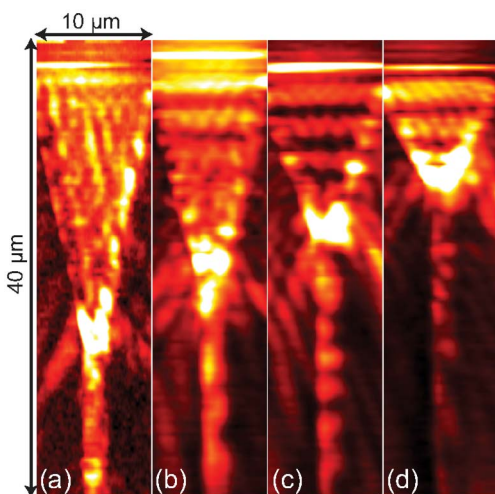


FIG. 2. (Color online) Near-field optical images of the tapering region for four different dimensions of the funnel in coupling at the free space excitation wavelength $\lambda=1520$ nm. (a) $10 \times 25 \mu\text{m}$ funnel, (b) $10 \times 20 \mu\text{m}$ funnel, (c) $10 \times 15 \mu\text{m}$ funnel, and (d) $10 \times 10 \mu\text{m}$ funnel.

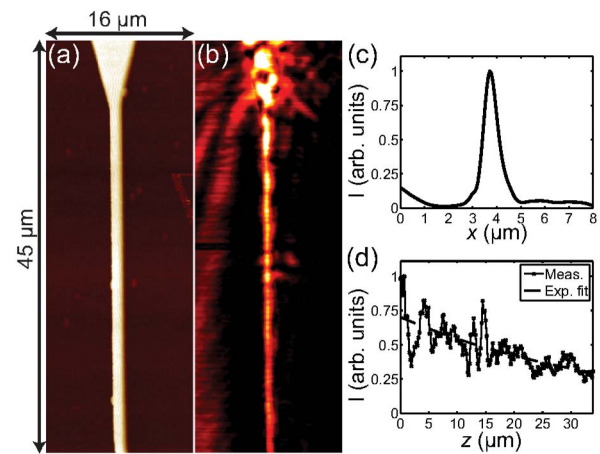


FIG. 3. (Color online) Near-field optical measurements of a straight DLSPPW with a $10 \times 25 \mu\text{m}$ in coupling funnel. [(a) and (b)] Topographical and near-field optical signal images, respectively, for $\lambda=1550$ nm. (c) Cross section of the optical image perpendicular to the waveguide and (d) averaged profile of the near-field optical signal recorded along the waveguide.

from tapering region to waveguide is found to be desirable.

Straight DLSPWs have been investigated at the telecommunication wavelength $\lambda=1550$ nm [Fig. 3]. The topography recorded with the fiber tip shows a smooth transition from the tapering region to the waveguide region, revealing only very small irregularities in the waveguide structure [Fig. 3(a)]. The image of the recorded near-field optical signal shows a highly confined DLSPW mode [Fig. 3(b)]. The cross section of the optical signal perpendicular to the waveguide yields a full width at half maximum of ~ 706 nm. Furthermore, it confirms that the tapering region, in addition to launching DLSPW modes, also reduces SPP propagation along the gold-air interface close to the waveguide [Fig. 3(c)]. An averaged profile of the optical signal taken along the ridge reveals a $1e$ propagation length of $\sim 39 \mu\text{m}$, determined from an exponential fit to the profile [Fig. 3(d)]. This value is lower than the propagation length of $50 \mu\text{m}$, expected from the numerical results,¹³ however, the discrepancy can be partly explained by radiation losses into the substrate due to the thin metal film, and scattering losses from small roughnesses in the dielectric ridge and gold surface, which were not included in the calculations. Other explanations for the discrepancy include statistical errors introduced in the exponential fit and possible variations of the permittivity of the gold film, caused by the deposition process. The absence of mode beating confirms that the DLSPPW indeed is single mode as expected from theoretical predictions.¹³

The confinement of the DLSPW modes has been investigated by characterizing S bends with different displacements [Fig. 4]. The recorded topographies show S bends resulting in a waveguide displacement of $5 \mu\text{m}$ [Fig. 4(b)] and $10 \mu\text{m}$ [Fig. 4(d)] over a distance of $10 \mu\text{m}$. In the case of the small S bend, characterized with the smallest curvature radius $R_{\text{min}} \approx 3.95 \mu\text{m}$, no significant bend loss can be observed from the optical image [Fig. 4(c)], and the strong scattering and back reflection at the termination of the waveguide [Fig. 4(g)] also imply low bend and propagation losses. From Figs. 4(c) and 4(e), it is clear that the size of the excitation spot ($\sim 15 \mu\text{m}$) is large enough to cause SPPs propagating parallel to the DLSPW at the gold-air interface, which then scatters off the DLSPW bend. This could, how-

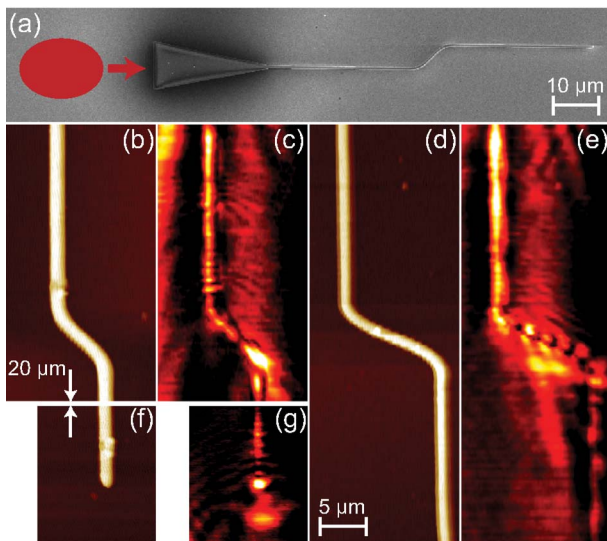


FIG. 4. (Color online) Near-field measurements of two different S bends, performed for $\lambda=1550$ nm. (a) SEM image of an S bend with $5\ \mu\text{m}$ displacement over a distance of $10\ \mu\text{m}$, where the ellipse illustrates the position of the excitation spot, and the arrow indicates the direction of SPP propagation. [(b) and (c)] Topographic and near-field optical images, respectively, of the S bend shown in (a). [(d) and (e)] Topographic and near-field optical images, respectively, of an S bend with a $10\ \mu\text{m}$ displacement over a distance of $10\ \mu\text{m}$. [(f) and (g)] Topographic and near-field optical images, respectively, of the termination region of the S bend shown in (a). The images in (b)–(g) all share the scale shown in (d).

ever, be avoided either by placing funnels adjacent to the one used for in coupling, as was the case with the straight waveguides [Fig. 1(a)], or by decreasing the spot size to funnel width ratio. The large bend reveals some radiation effects at the bends due to the very small radius of curvature ($R_{\text{min}} \approx 2.48\ \mu\text{m}$) of this bend [Fig. 4(e)]. Although some radiation losses occur, waveguiding can still be observed after the S bend, indicating very strong confinement of the DLSPPW modes.

In conclusion, it has been demonstrated, that it is possible to achieve strong mode confinement of SPPs at telecommunication wavelengths by utilizing ~ 550 -nm-high and ~ 500 -nm-wide dielectric ridges deposited on a thin gold film as waveguides. The use of a funnel structure for efficient in coupling of SPPs excited at the gold-air interface into DLSPPW modes is found advantageous, also because it reduces the propagation of SPPs at the gold-air interface adjacent to the waveguide. In addition to this, two S bends with different radii of curvature have been characterized, and it is found that a $5\ \mu\text{m}$ displacement over a distance of $10\ \mu\text{m}$ gives rise to very low radiation losses, confirming the strong confinement of the DLSPPW mode.

The authors acknowledge the financial support of the PLASMOCOM project (EC FP6 IST 034754 STREP).

- ¹W. L. Barnes, A. Dereux, and T. W. Ebbesen, *Nature (London)* **424**, 824 (2003).
- ²H. Raether, *Surface Plasmons—on Smooth and Rough Surfaces and on Gratings*, 1st ed. (Springer, Berlin, 1988).
- ³S. I. Bozhevolnyi, J. Erland, K. Leosson, P. M. W. Skovgaard, and J. M. Hvam, *Phys. Rev. Lett.* **86**, 3008 (2001).
- ⁴P. Berini, *Phys. Rev. B* **61**, 10484 (2000).
- ⁵T. Nikolajsen, K. Leosson, I. Salakhutdinov, and S. I. Bozhevolnyi, *Appl. Phys. Lett.* **82**, 668 (2003).
- ⁶A. Boltasseva, T. Nikolajsen, K. Leosson, K. Kjaer, M. S. Larsen, and S. I. Bozhevolnyi, *J. Lightwave Technol.* **23**, 413 (2005).
- ⁷I. V. Novikov and A. A. Maradudin, *Phys. Rev. B* **66**, 035403 (2002).
- ⁸D. K. Gramotnev and D. F. P. Pile, *Appl. Phys. Lett.* **85**, 6323 (2004).
- ⁹S. I. Bozhevolnyi, V. S. Volkov, E. Devaux, J.-Y. Laluet, and T. W. Ebbesen, *Nature (London)* **440**, 508 (2006).
- ¹⁰B. Steinberger, A. Hohenau, H. Ditlbacher, A. L. Stepanov, A. Drezet, F. R. Aussenegg, A. Leitner, and J. R. Krenn, *Appl. Phys. Lett.* **88**, 094104 (2006).
- ¹¹B. Steinberger, A. Hohenau, H. Ditlbacher, F. R. Aussenegg, A. Leitner, and J. R. Krenn, *Appl. Phys. Lett.* **91**, 081111 (2007).
- ¹²C. Reinhardt, S. Passinger, B. N. Chichkov, C. Marquart, I. P. Radko, and S. I. Bozhevolnyi, *Opt. Lett.* **31**, 1307 (2006).
- ¹³T. Holmgaard and S. I. Bozhevolnyi, *Phys. Rev. B* **75**, 245405 (2007).
- ¹⁴A. V. Krasavin and A. V. Zayats, *Appl. Phys. Lett.* **90**, 211101 (2007).